Applied Mathematical Modelling 38 (2014) 1001–1010

Contents lists available at ScienceDirect

Applied Mathematical Modelling

journal homepage: www.elsevier.com/locate/apm

Curved domain walls dynamics driven by magnetic field and electric current in hard ferromagnets

Giancarlo Consolo *, Carmela Currò, Giovanna Valenti

Department of Mathematics and Computer Science, University of Messina, V.le F. D'Alcontres, I-98166 Messina, Italy

ARTICLE INFO

Article history:
Received 3 September 2012
Received in revised form 20 June 2013
Accepted 16 July 2013
Available online 29 July 2013

Keywords:
Curved domain walls
Micromagnetism
Nonlinear dissipation
Reductive perturbation method
Spin-transfer-torque

ABSTRACT

The propagation of curved domain walls in hard ferromagnetic materials is studied by applying a reductive perturbation method to the generalized Landau–Lifshitz–Gilbert equation. The extended model herein considered explicitly takes into account the effects of a spin-polarized current as well as those arising from a nonlinear dissipation.

Under the assumption of steady regime of propagation, the domain wall velocity is derived as a function of the domain wall curvature, the nonlinear damping coefficient, the magnetic field and the electric current. Threshold and Walker-like breakdown conditions for the external sources are also determined. The analytical results are evaluated numerically for different domain wall surfaces (planes, cylinders and spheres) and their physical implications are discussed.

1. Introduction

In recent years, the properties of magnetic domain walls (DWs) observed in ferromagnetic materials have attracted a great deal of attention due to their fundamental interest and their potential technological applications in the fields of magnetic storage and logic devices. Many theoretical and experimental investigations performed on magnetic nanowires and nanostrips have indeed demonstrated that both static and dynamic information can be associated to the continuous transition layers between uniformly-magnetized adjacent regions, commonly referred to as DWs. In such devices, it was indeed shown that the information can be stored and transmitted by controlling, respectively, the structure and the motion of DWs [1,2].

In former papers [3–5], the one-dimensional dynamics of DWs in ferromagnetic nanostrips subject to the action of external magnetic fields and spin-polarized currents was analyzed on the basis of the extended Landau–Lifshitz–Gilbert (ELLG) equation [6,7]. This model, which describes the precessional motion of the magnetization vector in the framework of continuous media, incorporates both classical viscous dissipation and current-induced spin-torque effects. In [3], in particular, our attention was focused on the analytical and numerical characterization of magnetic materials which exhibit crystallographic defects, such as inclusions, impurities and dislocations. For this class of materials, the corresponding relaxation phenomena were characterized by generalizing the dissipation function through an additional dry-friction term [8,9]. By adopting the classical traveling waves ansatz, we deduced the expression of the DW velocity as a function of the external driving sources (magnetic fields and electric currents) and of the dry-friction strength. Our approach confirmed the existence of two dynamical regimes, steady-state and precessional, which are observed for different magnitudes of the external sources. Results of our analysis showed that, when dry-friction is included in the model, the steady DW motion takes place

* Corresponding author. Tel.: +39 090 3977556; fax: +39 090 3974170.
E-mail addresses: gconsolo@unime.it (G. Consolo), ccurro@unime.it (C. Currò), gvalenti@unime.it (G. Valenti).

0307-904X/$ - see front matter © 2013 Elsevier Inc. All rights reserved.
http://dx.doi.org/10.1016/j.apm.2013.07.032

for fields and currents which overcome well-defined threshold values and stops at the so-called Walker breakdown. Such theoretical results were also verified by numerical micromagnetic simulations.

It should be pointed out that such an investigation was carried out under the hypothesis that the DW surface is flat, with the normal to the plane parallel to the direction of propagation.

Nevertheless, some experimental [10–12] and theoretical [13–17] works showed that qualitatively different behaviors can be observed when the shape of the DW is curved.

Therefore, this paper aims to generalize our previous results to the case of curved DWs which are modeled through smoothly evolving surfaces. In particular, we consider ferromagnetic materials exhibiting a high magnetocrystalline anisotropy so that the DW width becomes an infinitesimal quantity and, consequently, the analysis can be carried out by means of a reductive perturbation method [18–21].

The present paper is organized as follows.

In Section 2, we briefly summarize the main results related to dynamics of flat DWs whose relaxation processes are described through a standard linear Gilbert dissipation model [22,23].

In Section 3, we focus our attention on a nonlinear dissipation model [24] and we look for solutions of the ELLG equation in the form of an asymptotic expansion around the equilibrium configuration. By means of this method, we derive a new formula for the velocity of curved DWs valid for external sources below the above mentioned Walker breakdown condition. Since we are essentially interested to hard ferromagnets, characterized by a large value of the dimensionless anisotropy parameter β (and, consequently, by a small DW thickness), we assume β of the order of ε^{-1}, being ε the small dimensionless expansion parameter. The results so obtained generalize those of [16] where an infinite ferromagnet was considered and the effects of spin torque and nonlinear dissipation were not included in the model.

In Section 4, the numerical evaluation of the results obtained is performed for some typologies of DW surfaces (planes, cylinders and spheres) and some concluding remarks are drawn.

2. Field equation and related classical results

In the present section, we briefly summarize the model equation on which our analysis is based and recall the main results obtained in the former paper [3].

Magnetization dynamics driven by a spin-polarized electric current in sub-micron scale ferromagnets, including the one-dimensional motion of DWs in thin wires or stripes, is described by the ELLG equation:

$$\dot{\mathbf{m}} = \gamma(\mathbf{h}_{\text{eff}} \wedge \mathbf{m}) + \mathbf{t}_{\text{d}} + \mathbf{t}_{\text{st}}. \tag{1}$$

which is the classical Landau–Lifshitz–Gilbert equation with an additional spin-transfer term accounting for the effect that conduction electrons exert on magnetization through the microscopic $s-d$ exchange interaction [6–22,24–29]. In (1), $\mathbf{m} = \frac{\mathbf{M}}{M_{\text{S}}}$ is the unit vector along the local magnetization, M_{S} the saturation magnetization and the over-dot denotes time derivation. The parameter $\gamma = M_{\text{S}}\mu_0\gamma_{\text{e}}$ is a constant expressed in terms of the magnetic permeability of the vacuum μ_0 and of the gyromagnetic ratio $\gamma_{\text{e}} = ge/m_{\text{e}}$, being g the Landè factor, e the electron charge and m_{e} the electron mass. The first term in the right-hand side of (1) describes conservative precession of the magnetization $\mathbf{m}$ about the direction of the effective magnetic field $\mathbf{h}_{\text{eff}}$, the second term $\mathbf{t}_{\text{d}}$ is the dissipative torque describing energy dissipation and the last term $\mathbf{t}_{\text{st}}$ represents the spin-transfer torque. The effective magnetic field $\mathbf{h}_{\text{eff}} = -\frac{\delta W}{\delta \mathbf{m}}$, calculated as variational derivative of the free energy W, accounts for external $\mathbf{h}_{\text{ext}}$, exchange $\mathbf{h}_{\text{exc}}$, demagnetizing $\mathbf{h}_{\text{dmg}}$ and anisotropy $\mathbf{h}_{\text{an}}$ fields:

$$\mathbf{h}_{\text{eff}} = \mathbf{h}_{\text{ext}} + \mathbf{h}_{\text{exc}} + \mathbf{h}_{\text{dmg}} + \mathbf{h}_{\text{an}}. \tag{2}$$

In the case of a medium of ellipsoidal shape and uniformly magnetized, the associate demagnetizing field, determined from the Maxwell equations by including the discontinuous jump of the magnetization at the body surface [30], is given by:

$$\mathbf{h}_{\text{dmg}} = -N_1(\mathbf{m}\cdot\mathbf{c}_1)\mathbf{c}_1 - N_2(\mathbf{m}\cdot\mathbf{c}_2)\mathbf{c}_2 - N_3(\mathbf{m}\cdot\mathbf{e})\mathbf{e}, \tag{3}$$

being $\{O, x_1, x_2, x_3\}$ a right-handed coordinate system of unit vectors $\{\mathbf{c}_1, \mathbf{c}_2, \mathbf{c}_3\}$, $\mathbf{e} \equiv \mathbf{c}_3$ the direction along which the magnetization minimizes the system free energy (the so-called "easy axis"), whereas N_1, N_2 and N_3 are the demagnetizing factors satisfying the normalization condition $N_1 + N_2 + N_3 = 1$. We would like to remark that the expression of $\mathbf{h}_{\text{dmg}}$ (3) is commonly used in literature as a good approximation also for non ellipsoidal bodies by retaining the only diagonal terms of the corresponding tensor [30]–[32].

The exchange $\mathbf{h}_{\text{exc}}$ and the anisotropy $\mathbf{h}_{\text{an}}$ fields have the following expressions:

$$\begin{aligned} \mathbf{h}_{\text{exc}} &= A\Delta\mathbf{m}, \\ \mathbf{h}_{\text{an}} &= \beta(\mathbf{m}\cdot\mathbf{e})\mathbf{e} \end{aligned} \tag{4}$$

where Δ is the laplacian operator while the constants A and β are related to the anisotropy constant K and the exchange stiffness constant A_{ex}, respectively, through the relations:

$$\beta = \frac{2K}{\mu_0 M_{\text{S}}^2}, \quad A = \frac{2A_{\text{ex}}}{\mu_0 M_{\text{S}}^2}. \tag{5}$$

The most general phenomenological form of the damping term, under the assumptions that dissipation is isotropic and local, is given by the Gilbert-like damping torque [23,24]:

$$\mathbf{t}_{\mathrm{d}} = \alpha\left(\dot{\mathbf{m}}^2\right)\left(\mathbf{m}\wedge\dot{\mathbf{m}}\right) \tag{6}$$

with $\alpha\left(\dot{\mathbf{m}}^2\right)$ a positive-definite dimensionless function which, for finite but not very large angles of magnetization precession, can be represented as a Taylor series expansion [24]:

$$\alpha\left(\dot{\mathbf{m}}^2\right) = \alpha_{\mathrm{G}}\sum_{j\geqslant 0} q_j\left(\gamma^{-1}\dot{\mathbf{m}}\right)^{2j}, \quad q_0 = 1. \tag{7}$$

where q_j are dimensionless coefficients.

The spin transfer torque $\mathbf{t}_{\mathrm{st}}$ is not derivable from a potential but its form is fixed by symmetry arguments and model calculations [33]. A local approximation is:

$$\mathbf{t}_{\mathrm{st}} = (-1+\eta\mathbf{m}\wedge)(\mathbf{u}\cdot\nabla)\mathbf{m} \tag{8}$$

where η is the phenomenological non-adiabatic spin transfer parameter [6–22,24–29]. The velocity $\mathbf{u}$ is a vector along the direction of the electron motion with an amplitude $u = \left(gJ_{\mathrm{e}}\mu_{\mathrm{B}}P/2eM_{\mathrm{S}}\right)$ being μ_{B} the Bohr magneton, J_{e} the current density and P the polarization factor of the current.

In order to recall the main classical results related to the dynamics of DWs having flat surfaces, let us consider, as in our previous paper [3], a nanostrip of length L, width w and thickness d with $L \gg w > d$. We assume the x_3 (easy) axis to be along the perpendicular to the strip axis (x_1 axis), the external magnetic field to be uniform in space, constant in time and directed along the easy axis and an electric current to flow along the wire axis, namely:

$$\begin{aligned}\mathbf{h}_{\mathrm{ext}} &= h\mathbf{e}\\ \mathbf{t}_{\mathrm{st}} &= u(-1+\eta\mathbf{m}\wedge)\frac{\partial\mathbf{m}}{\partial x_1}.\end{aligned} \tag{9}$$

If the dissipation processes are taken into account by means of the basic zeroth-order approximation of (7), namely $\alpha\left(\dot{\mathbf{m}}^2\right) = \alpha_{\mathrm{G}} = const.$, it is possible to obtain a traveling wave solution of the form [34,35]:

$$\mathbf{m}(x_1,t) = -\tanh\frac{x_1-\lambda t}{\delta}\mathbf{e} + \frac{1}{\cosh\frac{x_1-\lambda t}{\delta}}(\cos\varphi_0\mathbf{c}_1 + \sin\varphi_0\mathbf{c}_2). \tag{10}$$

In (10), $\varphi_0 = const$ represents the azimuthal angle related to $\mathbf{m}$, δ is the wall width whereas λ is the constant DW velocity. Their expressions are given, respectively, by:

$$\sin 2\varphi_0 = \frac{2\left[h+\frac{u}{\gamma\delta}(\eta-\alpha_{\mathrm{G}})\right]}{\alpha_{\mathrm{G}}(N_1-N_2)} \tag{11}$$

$$\delta = \sqrt{\frac{A}{\beta+N_2-N_3+(N_1-N_2)\cos^2\varphi_0}} \tag{12}$$

$$\lambda = \frac{u}{\alpha_{\mathrm{G}}}\eta + \frac{h\gamma}{\alpha_{\mathrm{G}}}\delta \tag{13}$$

The relation (11) allows us to deduce the Walker breakdown values for the external magnetic field and the current density when these sources act separately:

$$\begin{aligned}u = 0 &\Rightarrow h_{\mathrm{w}} = \frac{\alpha_{\mathrm{G}}}{2}|N_1-N_2|\\ h = 0 &\Rightarrow u_{\mathrm{w}} = \frac{\gamma\delta\alpha_{\mathrm{G}}|N_1-N_2|}{2|\eta-\alpha_{\mathrm{G}}|}\end{aligned} \tag{14}$$

which set an upper limit on the maximum value of the DW velocity achievable in the steady-state regime.

It should be noticed that, in the framework of flat DWs and Gilbert damping, the motion takes place for any non-null value of the source terms, namely there are no threshold conditions.

The explicit solution (10) of the ELLG equation also points out that the wall thickness δ is a material parameter which plays a crucial role in the DW dynamics. Therefore, a meaningful comparison between experiment and theory requires a more realistic representation of the domain structure to which the next section is devoted.

3. Curved domain walls dynamics

In this section we model the DW by means of a regular surface $\Sigma(t)$ of cartesian equation $\phi(x_1,x_2,x_3,t) = 0$ such that the normal speed of propagation λ, the unit normal vector $\mathbf{n}$ to $\Sigma(t)$ and the mean curvature κ of the DW are given, respectively, by:

$$\lambda = -\frac{\frac{\partial \phi}{\partial t}}{|\nabla \phi|}, \quad \mathbf{n} = \frac{\nabla \phi}{|\nabla \phi|}, \quad \kappa = \nabla \cdot \mathbf{n}. \tag{15}$$

Furthermore, we assume a nonlinear model of dissipation [24], obtained by considering the first-order approximation of (7), namely:

$$\alpha\left(\dot{\mathbf{m}}^2\right) = \alpha_G\left(1 + \frac{q_1}{\gamma^2}\dot{\mathbf{m}}^2\right) \tag{16}$$

so that the ELLG Eq. (1) becomes:

$$\dot{\mathbf{m}} - \alpha_G\left(1 + \frac{q_1}{\gamma^2}\dot{\mathbf{m}}^2\right)\left(\mathbf{m} \wedge \dot{\mathbf{m}}\right) = \gamma \mathbf{h}_{\text{eff}} \wedge \mathbf{m} + (-1 + \eta \mathbf{m} \wedge)(\mathbf{u} \cdot \nabla)\mathbf{m} \tag{17}$$

with

$$\mathbf{h}_{\text{eff}} = A\Delta \mathbf{m} + \beta(\mathbf{m} \cdot \mathbf{e})\mathbf{e} - N_1(\mathbf{m} \cdot \mathbf{c}_1)\mathbf{c}_1 - N_2(\mathbf{m} \cdot \mathbf{c}_2)\mathbf{c}_2 - N_3(\mathbf{m} \cdot \mathbf{e})\mathbf{e} + \mathbf{h}_{\text{ext}}. \tag{18}$$

In order to derive, by means of a formal asymptotic analysis, a theoretical formula for the velocity of a curved DW which moves along a ferromagnet of finite dimensions, we need to introduce first the following dimensionless variables and parameters:

$$\begin{aligned} &\widetilde{\mathbf{x}} = L^{-1}\mathbf{x}, \quad \widetilde{t} = T^{-1}t, \quad \widehat{\lambda} = TL^{-1}\lambda, \quad \widehat{\kappa} = L\kappa, \\ &\widehat{\gamma} = T\gamma, \quad \widehat{A} = L^{-2}A \quad \widehat{\mathbf{u}} = TL^{-1}\mathbf{u} \end{aligned} \tag{19}$$

where $\mathbf{x} = (x_1, x_2, x_3)$, and L and T are suitable length and time scales. Consequently, the (17) reads:

$$\frac{\widehat{\delta}}{\beta \widehat{v}}\left[\alpha_G^{-1}\frac{\partial \mathbf{m}}{\partial \widetilde{t}} - \left(1 + \frac{q_1}{\widehat{\gamma}^2}\left|\frac{\partial \mathbf{m}}{\partial \widetilde{t}}\right|^2\right)\mathbf{m} \wedge \frac{\partial \mathbf{m}}{\partial \widetilde{t}}\right] = \left[\widehat{\delta}^2 \widetilde{\Delta}\mathbf{m} + (\mathbf{m} \cdot \mathbf{e})\mathbf{e} + +\beta^{-1}\left(\mathbf{h}_{\text{dmg}} + \mathbf{h}_{\text{ext}} - \frac{\mathbf{m}}{\widehat{\gamma}} \wedge \left(\widehat{\mathbf{u}} \cdot \widetilde{\nabla}\right)\mathbf{m} - \frac{\eta}{\widehat{\gamma}}\left(\widehat{\mathbf{u}} \cdot \widetilde{\nabla}\right)\mathbf{m}\right)\right] \wedge \mathbf{m} \tag{20}$$

with

$$\widehat{\delta} = \left(\frac{\widehat{A}}{\beta}\right)^{1/2}, \quad \widehat{v} = \frac{\widehat{\delta}}{\alpha_G}\widehat{\gamma}. \tag{21}$$

Since we are interested to the class of hard ferromagnetic materials, characterized by a very large anisotropy energy, we introduce the small parameter

$$\epsilon = \beta^{-1} \tag{22}$$

so that $\widehat{\delta}$ becomes smaller as the anisotropy coefficient βincreases. It is straightforward to notice that, under the hypothesis (22), from (12) $\widehat{\delta}$ turns out to be the dimensionless DW thickness. Accordingly, we choose the time and the length scales, T and L, as follows:

$$T = \epsilon^{-1}\frac{1}{\gamma}, \quad L = \epsilon^{-1/2}A^{1/2}, \tag{23}$$

in turn we have

$$\widehat{\delta} = \epsilon, \quad \widehat{v} = (\alpha_G)^{-1}. \tag{24}$$

By taking into account (22) and (23), and dropping $\widetilde{}$ for notation convenience, the Eq. (20) becomes:

$$\begin{aligned} &\epsilon^2\left(\frac{\partial \mathbf{m}}{\partial t} - \alpha_G\left(1 + \epsilon^2 q_1\left|\frac{\partial \mathbf{m}}{\partial t}\right|^2\right)\left(\mathbf{m} \wedge \frac{\partial \mathbf{m}}{\partial t}\right)\right) = \\ &\left[\epsilon^2\left(\Delta \mathbf{m} - \mathbf{m} \wedge \left(\widehat{\mathbf{u}} \cdot \nabla\right)\mathbf{m} - \eta\left(\widehat{\mathbf{u}} \cdot \nabla\right)\mathbf{m}\right) + \epsilon\left(\mathbf{h}_{\text{dmg}} + \mathbf{h}_{\text{ext}}\right) + (\mathbf{m} \cdot \mathbf{e})\mathbf{e}\right] \wedge \mathbf{m} \end{aligned} \tag{25}$$

which points out that the magnetization dynamics is governed by terms of different order. In particular, we can easily see that when $\epsilon$is small, all the dissipative effects (damping and spin-transfer torque) together with the conservative contributions arising from exchange, demagnetizing and external fields, become negligible with respect to the anisotropy interactions. This means that, in a short time, in each of magnetic domains, $\mathbf{m}$ orientates nearly parallel to $\mathbf{e}$.

In what follows, by looking for an asymptotic solution of (25) exhibiting the feature of a progressive wave, we will assume that $\mathbf{m}$ can be expanded in powers of ϵ

$$\begin{aligned}&\mathbf{m}=\mathbf{m}_0(x_1,x_2,x_3,t,z)+\sum_{j>0}\epsilon^j\mathbf{m}_j(x_1,x_2,x_3,t,z),\\&z=\epsilon^{-1}\phi(x_1,x_2,x_3,t)\\&\lim_{z\to\pm\infty}\mathbf{m}_0=\pm\mathbf{e},\quad \lim_{z\to\pm\infty}\mathbf{m}_j=\mathbf{0},\quad j>0.\end{aligned}\tag{26}$$

being $\mathbf{m}_0$ and $\mathbf{m}_j$ $(j>0)$ the coefficients of the power expansion.

Since all the solutions of the ELLG equation must have constant modulus, expansion (26) is consistent with such a requirement if

$$|\mathbf{m}_0|=1,\quad \sum_{i=0}^{j}\mathbf{m}_i\cdot\mathbf{m}_{j-i}=0,\quad j\geqslant 1.\tag{27}$$

After inserting (26) into (25), and requiring the coefficients of the different powers of $\epsilon$to be termwise zero, we obtain the following set of conditions of the orders ϵ^0 and ϵrespectively

$$\begin{aligned}&\mathbf{m}_0\wedge\left(\frac{\partial^2\mathbf{m}_0}{\partial z^2}+(\mathbf{e}\cdot\mathbf{m}_0)\mathbf{e}\right)=\mathbf{0}\\&\mathbf{m}_1\wedge\left[\frac{\partial^2\mathbf{m}_0}{\partial z^2}+(\mathbf{e}\cdot\mathbf{m}_0)\mathbf{e}\right]+\mathbf{m}_0\wedge\left[\frac{\partial^2\mathbf{m}_1}{\partial z^2}+(\mathbf{e}\cdot\mathbf{m}_1)\mathbf{e}\right]+\mathbf{b}_0=\mathbf{0}\end{aligned}\tag{28}$$

where, without loss of generality, we assumed $|\nabla\phi|=1$ and where $\mathbf{b}_0$ is given by:

$$\mathbf{b}_0=\left(\widehat{\mathbf{u}}\cdot\mathbf{n}-\widehat{\lambda}\right)\frac{\partial\mathbf{m}_0}{\partial z}+\mathbf{m}_0\wedge\left[\mathbf{h}_{\mathrm{dmg}_0}+\mathbf{h}_{\mathrm{ext}}+\left(\alpha_G\widehat{\lambda}\left(1+q_1\left|\frac{\partial\mathbf{m}_0}{\partial z}\right|^2\widehat{\lambda}^2\right)-\eta\widehat{\mathbf{u}}\cdot\mathbf{n}+\widehat{\kappa}\right)\frac{\partial\mathbf{m}_0}{\partial z}\right]\tag{29}$$

being $\mathbf{h}_{\mathrm{dmg}_0}$ the lowest order approximation of the Eq. (3), that is

$$\mathbf{h}_{\mathrm{dmg}_0}=-N_1(\mathbf{m}_0\cdot\mathbf{c}_1)\mathbf{c}_1-N_2(\mathbf{m}_0\cdot\mathbf{c}_2)\mathbf{c}_2-N_3(\mathbf{m}_0\cdot\mathbf{e})\mathbf{e}.\tag{30}$$

We would like to stress that in (30) we made the approximation of considering the demagnetizing factors not affected by the time evolution of the DW surface. Such an assumption is necessary in view of the complexity in the determination of the exact values of the demagnetizing coefficients for bodies of arbitrary shape. However, keeping in mind that each of these coefficients is inversely proportional to the corresponding dimension of the DW region, being in our case the DW thickness (of order ϵ) very small compared to the other lateral sizes, no significant variations of these parameters are expected and, in turn, our hypothesis appears to be more than justifiable.

Since the Eqs. (28) are formally the same as those obtained in [16], the smooth solutions to problem $(28)_1$, with boundary conditions $(26)_3$, assume the form:

$$\mathbf{m}_0(\mathbf{x},t,z)=\tanh(z-\omega)\mathbf{e}+\frac{1}{\cosh(z-\omega)}(\cos\psi\mathbf{c}_1+\sin\psi\mathbf{c}_2)\tag{31}$$

being $\omega(\mathbf{x},t)$ and $\psi(\mathbf{x},t)$ suitable fields. As it is easy to ascertain, when $\Sigma(t)$is a plane with unit normal $\mathbf{c}_1$ parallel to the easy axis $\mathbf{e}$, that is $\phi=x_1-\lambda t$, if we choose $\omega=0$ and $\psi=\varphi_0$, the (31) recovers exactly the solution (10) previously obtained where, as a consequence of (22), the DW width δreduces to $\left(\frac{A}{\beta}\right)^{1/2}$.

On the other hand, from $(28)_2$, two solvability conditions can be derived. More precisely, by performing the cross product of both sides of $(28)_2$ by $\mathbf{m}_0$, we get:

$$\left[\mathbf{m}_0\cdot\left(\frac{\partial^2\mathbf{m}_1}{\partial z^2}+(\mathbf{e}\cdot\mathbf{m}_1)\mathbf{e}\right)\right]\mathbf{m}_0-\frac{\partial^2\mathbf{m}_1}{\partial z^2}-(\mathbf{e}\cdot\mathbf{m}_1)\mathbf{e}+\left[\mathbf{m}_0\cdot\left(\frac{\partial^2\mathbf{m}_0}{\partial z^2}+(\mathbf{e}\cdot\mathbf{m}_0)\mathbf{e}\right)\right]\mathbf{m}_1+\mathbf{m}_0\wedge\mathbf{b}_0=\mathbf{0}.\tag{32}$$

Then, by taking the scalar product of (32) with $\frac{\partial\mathbf{m}_0}{\partial z}$ and $\mathbf{m}_0\wedge\mathbf{e}$, we obtain respectively:

$$(\mathbf{b}_0\wedge\mathbf{m}_0)\cdot\frac{\partial\mathbf{m}_0}{\partial z}+\frac{\partial}{\partial z}\left(\frac{\partial\mathbf{m}_1}{\partial z}\cdot\frac{\partial\mathbf{m}_0}{\partial z}-\mathbf{m}_1\cdot\frac{\partial^2\mathbf{m}_0}{\partial z^2}\right)=0\tag{33}$$

$$(\mathbf{b}_0\wedge\mathbf{m}_0)\cdot(\mathbf{m}_0\wedge\mathbf{e})+\mathbf{e}\cdot\frac{\partial}{\partial z}\left(\frac{\partial\mathbf{m}_1}{\partial z}\wedge\mathbf{m}_0+\frac{\partial\mathbf{m}_0}{\partial z}\wedge\mathbf{m}_1\right)=0\tag{34}$$

where the following identity, resulting from manipulation of $(28)_1$, has been considered:

$$\left[\frac{\partial^3\mathbf{m}_0}{\partial z^3}+\left(\mathbf{e}\cdot\frac{\partial\mathbf{m}_0}{\partial z}\right)\mathbf{e}-\left(\mathbf{m}_0\cdot\frac{\partial^2\mathbf{m}_0}{\partial z^2}+(\mathbf{e}\cdot\mathbf{m}_0)^2\right)\frac{\partial\mathbf{m}_0}{\partial z}\right]\cdot\mathbf{m}_1=0.\tag{35}$$

The integration of (33) and (34) over the real line, using $(26)_3$, allows to deduce the above mentioned solvability conditions:

$$\int_{-\infty}^{+\infty} \mathbf{m}_0 \wedge \mathbf{b}_0 \cdot \frac{\partial \mathbf{m}_0}{\partial z} dz = 0, \tag{36}$$

$$\int_{-\infty}^{+\infty} (\mathbf{m}_0 \wedge \mathbf{b}_0) \cdot (\mathbf{m}_0 \wedge \mathbf{e}) dz = 0. \tag{37}$$

which, taking into account $(26)_3$, (29) and (31), lead to respectively

$$\begin{aligned} &\alpha_G \left(1 + \frac{2}{3} q_1 \widehat{\lambda}^2\right) \widehat{\lambda} - \eta (\widehat{\mathbf{u}} \cdot \mathbf{n}) + \widehat{\kappa} + \mathbf{h}_{ext} \cdot \mathbf{e} = 0 \\ &2\left(\widehat{\mathbf{u}} \cdot \mathbf{n} - \widehat{\lambda}\right) + \pi(\cos\psi \mathbf{c}_2 - \sin\psi \mathbf{c}_1) \cdot \mathbf{h}_{ext} + (N_1 - N_2) \sin 2\psi = 0. \end{aligned} \tag{38}$$

Finally, by expressing (38) in the original physical variables, we obtain:

$$v^{-1} \left(\lambda + \frac{2}{3} \frac{\beta}{A} \frac{q_1}{\gamma^2} \lambda^3 - \frac{\eta}{\alpha_G} \mathbf{u} \cdot \mathbf{n}\right) + \sigma\kappa + \mathbf{h}_{ext} \cdot \mathbf{e} = 0 \tag{39}$$

$$2(\alpha_G v)^{-1} (\mathbf{u} \cdot \mathbf{n} - \lambda) + \pi(\cos\psi \mathbf{c}_2 - \sin\psi \mathbf{c}_1) \cdot \mathbf{h}_{ext} + (N_1 - N_2) \sin 2\psi = 0 \tag{40}$$

with

$$\sigma = (A\beta)^{1/2}, \quad v^{-1} = \frac{\alpha_G}{\gamma} \sqrt{\frac{\beta}{A}} \tag{41}$$

By taking into account (15), the partial differential equation (39) describes the evolution of the curved DW surface $\phi(x_1, x_2, x_3, t)$which strongly depends upon all the conservative and dissipative effects here considered. On the other hand, Eq. (40) affects $\psi(x_1, x_2, x_3, t)$and hence provides information on the zeroth-order magnetization.

In the particular case of a domain wall surface translating rigidly along a preferred axis with a constant velocity (the hypothesis of the so-called "steady dynamical regime" illustrated in the next section), the (39) gives the steady velocity as a function of the spin current density, the nonlinear damping and the mean curvature of the surface. In this framework, (40) provides information about the thresholds and the breakdown conditions on the driving sources, as it will be specified in the next section.

We also remark that Eqs. (39) and (40) generalize the results previously obtained in [16] where a linear damping model ($q_1 = 0$) and an infinite medium ($N_1 = N_2 = 0, N_3 = 1$) were considered in the absence of current-driven spin-transfer torque ($u = 0$).

Moreover, if we consider $\Sigma(t)$ to be a plane with unit normal $\mathbf{c}_1$ parallel to the easy axis $\mathbf{e}$, by assuming $(9)_1$ and the zeroth-order approximation of (7), the Eqs. (39) and (40) recover the classical solution (13) and (11), respectively.

4. Numerical results and final remarks

In this section, as illustrative examples of the general analytical results developed above, we assume to model the curved DW through constant-curvature surfaces, namely spheres and cylinders. Since the analysis is performed within the so-called "steady dynamical regime", in which the DW surface translates rigidly along the nanostrip axis with a constant velocity, the (39) and (40) can be treated as algebraic equations.

We consider a ferromagnetic nanostrip having width $w = 60$ nm and thickness $d = 20$ nm. In order to characterize a hard ferromagnet, we consider the typical parameters of a $SmCo_5$ alloy as in [30], namely: anisotropy constant $K = 1.7 \times 10^7$ J/m^3, saturation magnetization $M_S = 8.35 \times 10^5$ A/m, exchange constant $A_{ex} = 2.4 \times 10^{-11}$ J/m, dimensionless Gilbert damping constant $\alpha_G = 0.2$, current polarization factor $P = 0.5$ and non-adiabatic spin transfer parameter $\eta = 0.5$.

According to this setup, the DW width is $\delta = 1.18$ nm so that, by using the procedures described in [31,32], we deduced the following values of the demagnetizing factors $N_1 = 0.94, N_2 = 0.01, N_3 = 0.05$ which correspond to those of an ellipsoid of axes δ, w, d.

We also consider the external field and the electric current to be directed along the easy axis, namely $\mathbf{h}_{ext} = -h\mathbf{e}$ and $\mathbf{u} = u(J_e)\mathbf{e}$, so that the DW moves towards the positive easy axis and the Eqs. (39) and (40) reduce to:

$$\begin{aligned} &\frac{2}{3} \frac{\beta}{A} \frac{q_1}{\gamma^2} \lambda^3 + \lambda + v(\sigma\kappa - h) - \frac{\eta u}{\alpha_G} n_3 = 0 \\ &\sin 2\psi = \frac{2(\alpha_G v)^{-1} (u n_3 - \lambda)}{N_2 - N_1}. \end{aligned} \tag{42}$$

As it is easy to ascertain, since physically relevant DW velocities must obey the restriction $\lambda \geqslant 0$, from $(42)_1$ we have:

$$v(\sigma\kappa - h) - \frac{\eta u}{\alpha_G} n_3 \leqslant 0 \tag{43}$$

whereas $(42)_2$ leads to

$$un_3 - \frac{\alpha_G v|N_2 - N_1|}{2} \leqslant \lambda \leqslant un_3 + \frac{\alpha_G v|N_2 - N_1|}{2}. \tag{44}$$

More precisely, (43) determines a threshold condition for h and u below which no DW motion takes place while (44) defines the upper and the lower breakdown velocities that limit the motion in the steady-state regime.

In order to emphasize the different responses of the system herein considered under the action of applied magnetic fields and electric currents, we show the behavior of DW velocity when these external sources act separately.

The dependence of DW velocity λon the applied magnetic field h, in the absence of electric current, is shown in 1,2 in the cases of linear ($q_1 = 0$) and nonlinear ($q_1 \neq 0$) damping model, respectively.

In the present case, being $u = 0$, the left implication of (44) is trivially satisfied, whereas the breakdown velocity λ_W and the corresponding field h_W , obtained from $(42)_1$, are:

$$\lambda_W = \frac{\gamma}{2}\sqrt{\frac{A}{\beta}}|N_2 - N_1|$$
$$h_W = \frac{\alpha_G}{2}|N_2 - N_1|\left[1 + \frac{1}{6}q_1(N_2 - N_1)^2\right] + \sigma\kappa. \tag{45}$$

Figs. 1 and 2 show that the curvature of the DW surface introduces a threshold below which no DW motion is observed. As it is expected from (43), such a threshold value increases with curvature but is independent of the nonlinear damping coefficient, being $h_{th} = \sigma\kappa$. Such a behavior is illustrated in both figures where, once the geometry of the DW surface is fixed, the decrease of the radius of curvature R leads to a shift of the threshold towards larger values of the applied field. An analogous shift takes place by considering a cylinder and a sphere with the same radius of curvature. It should be noticed that any variation of the nonlinear damping coefficient q_1 does not affect such a threshold, as sketched for the spherical case in Fig. 2.

Then, from the comparison between Fig.1 and Fig.2, it is possible to appreciate the effects of the curvature of the DW and of the nonlinear damping with respect to the classical cases of flat DW and Gilbert damping. In particular, once the threshold is overcome, for a given nonlinear damping coefficient, a non-null curvature acts in such a way the DW velocity is shifted towards larger values of the driving force, i.e. $\lambda(h)|_{\kappa\neq 0} = \lambda(h - h_{th})|_{\kappa=0}$. In other words, if the DW geometry bends and deviates from the flat case, it is necessary to apply stronger external fields in order to reach a given DW velocity.

Furthermore, the dashed lines, which denote the upper breakdown velocity according to $(45)_1$, point out that the maximum value of the DW velocity is independent of both curvature and damping coefficients.

Let us consider now the behavior of the DW velocity under an applied current $u(J_e)$ only, which is sketched in Figs. 3,4.

In the present case, being $h = 0$, from (43) we obtain the following threshold for u:

$$u_{th} = \frac{\gamma}{\eta n_3}\sqrt{\frac{A}{\beta}}\sigma\kappa \tag{46}$$

which is curvature-dependent and damping-independent as in the field-driven case. However, differently from the previous case, the left implication of (44) leads to further restrictions on the threshold and the breakdown values for u.

Therefore, for the sake of clarity, we illustrate separately the applied current dependence of the DW velocity for the two above considered damping models.

Firstly, let us discuss the case of a linear damping model. Being $q_1 = 0$, the required compatibility conditions between $(42)_1$ and (44) define the lower and the upper breakdown for u and λ whose expressions are, respectively, given by:

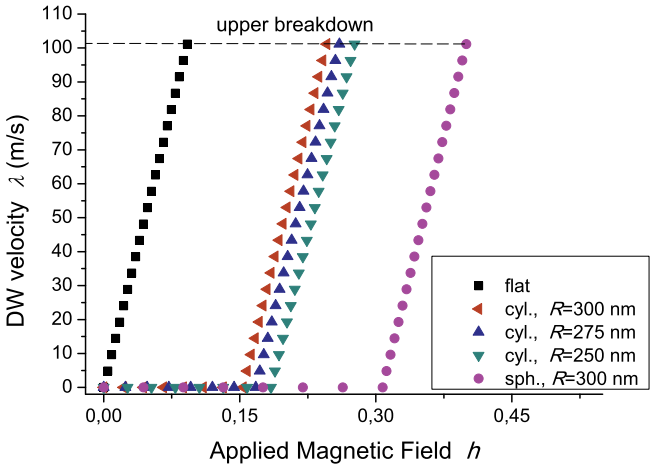

Fig. 1. Magnetic field dependence of the DW velocity for flat, cylindrical and spherical surfaces with different radii of curvature in the case of classical Gilbert damping ($q_1 = 0$). The dashed line represents the constant upper breakdown DW velocity.

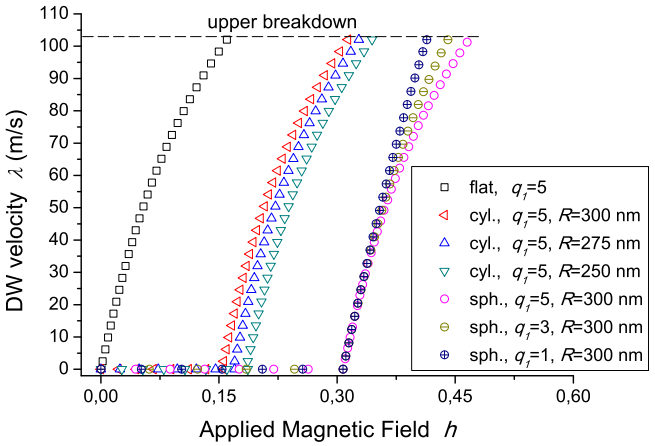

Fig. 2. Magnetic field dependence of the DW velocity for flat, cylindrical and spherical surfaces with different radii of curvature in the case of nonlinear damping ($q_1 \neq 0$). For the spherical geometry, such a dependence is evaluated for different nonlinear damping coefficients. The dashed line represents the constant upper breakdown DW velocity.

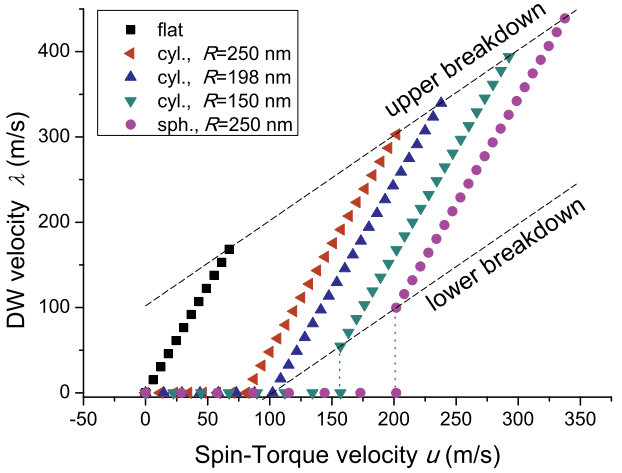

Fig. 3. Current-induced spin-torque dependence of the DW velocity for flat, cylindrical and spherical surfaces with different radii of curvature in the case of classical Gilbert damping ($q_1 = 0$). The dashed lines represent the lower and the upper breakdown DW velocities while the dotted lines stand for the jumps of the velocity occurring at $u_{\mathrm{W}}^{(low)}$.

$$
\begin{aligned}
\lambda_{\mathrm{W}}^{(low)} &= \frac{\gamma}{\eta-\alpha_{\mathrm{G}}}\sqrt{\frac{A}{\beta}}\left[\sigma\kappa-\frac{\eta}{2}|N_2-N_1|\right],\\
u_{\mathrm{W}}^{(low)} &= \frac{\gamma}{\eta-\alpha_{\mathrm{G}}}\sqrt{\frac{A}{\beta}}\left[\sigma\kappa-\frac{\alpha_{\mathrm{G}}}{2}|N_2-N_1|\right],\\
\lambda_{\mathrm{W}}^{(upp)} &= \frac{\gamma}{\eta-\alpha_{\mathrm{G}}}\sqrt{\frac{A}{\beta}}\left[\sigma\kappa+\frac{\eta}{2}|N_2-N_1|\right],\\
u_{\mathrm{W}}^{(upp)} &= \frac{\gamma}{\eta-\alpha_{\mathrm{G}}}\sqrt{\frac{A}{\beta}}\left[\sigma\kappa+\frac{\alpha_{\mathrm{G}}}{2}|N_2-N_1|\right].
\end{aligned}
\tag{47}
$$

By comparing (46) with $(47)_2$ we deduce the meaningful value of the effective threshold $u_{\mathrm{th}}^{*}=\max\left\{u_{\mathrm{th}},u_{\mathrm{W}}^{(low)}\right\}$ which only depends on the mean curvature κ once the geometry of the sample and the material parameters are fixed. In particular, in the illustrative example herein considered, owing to the choice $\eta>\alpha_{\mathrm{G}}$, if $\kappa<\frac{\eta}{2\sigma}|N_2-N_1|$, it follows that $u_{\mathrm{th}}^{*}=u_{\mathrm{th}}$ and the DW velocity increases smoothly starting from $\lambda=0$ to $\lambda=\lambda_{\mathrm{W}}^{(upp)}$. On the contrary, if $\kappa>\frac{\eta}{2\sigma}|N_2-N_1|$, the DW velocity exhibits a jump at the threshold $u_{\mathrm{th}}^{*}=u_{\mathrm{W}}^{(low)}$ from $\lambda=0$ to $\lambda=\lambda_{\mathrm{W}}^{(low)}$.

These different situations are illustrated in Fig. 3 where $u_{\mathrm{th}}^{*}=u_{\mathrm{th}}$ is represented for flat (■) and cylindrical (◀) DWs, while $u_{\mathrm{th}}^{*}=u_{\mathrm{W}}^{(low)}$ is depicted for cylindrical (▼) and spherical (●) DWs. Moreover, the case of a cylindrical (▲) DW corresponds to the limit condition $u_{\mathrm{th}}=u_{\mathrm{W}}^{(low)}$.

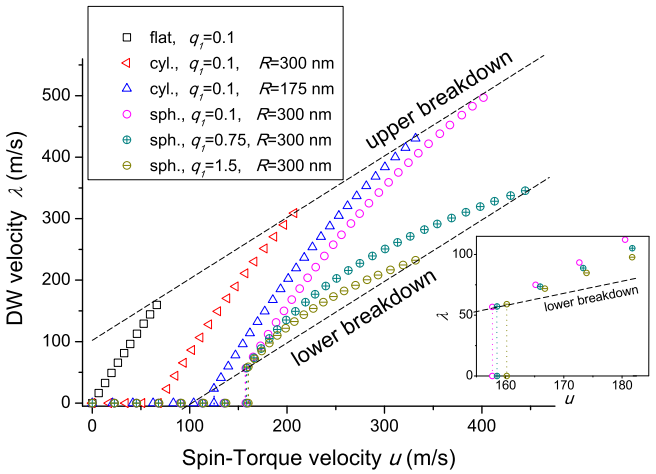

Fig. 4. Main panel: current-induced spin-torque dependence of the DW velocity for flat, cylindrical and spherical surfaces with different radii of curvature in the case of nonlinear damping. For the spherical geometry, such a dependence is evaluated for different nonlinear damping coefficients. The dashed lines represent the lower and the upper breakdown DW velocities while the dotted lines stand for the jumps of the velocity occurring at $u_W^{(low)}$. Inset: a zoom of the threshold region for the spherical geometry showing the velocity jumps and the dependence of the threshold value on the nonlinear damping coefficient.

Fig. 3 also shows that, for $u > u_{th}^*$, the DW velocity shifts towards larger values of the applied current for increasing mean curvatures, as it occurs in the field-driven case. Nevertheless, differently from that case, the upper breakdown is not constant anymore but depends on κ, as it is expected from $(47)_3$.

Let us discuss now the DW dynamics occurring when a nonlinear damping model is considered. By combining (42) with (44), the lower and the upper breakdown conditions become:

$$\begin{cases} u_W^{(low)} n_3 = \lambda_W^{(low)} + \frac{\gamma}{2}\sqrt{\frac{A}{\beta}}|N_2 - N_1| \\ \frac{2}{3}\frac{\beta}{A}\frac{q_1}{\gamma^2}\left(\lambda_W^{(low)}\right)^3 + \frac{\alpha_G - \eta}{\alpha_G}\lambda_W^{(low)} + \frac{\gamma}{\alpha_G}\sqrt{\frac{A}{\beta}}\left(\sigma\kappa - \frac{\eta}{2}|N_2 - N_1|\right) = 0 \end{cases} \tag{48}$$

$$\begin{cases} u_W^{(upp)} n_3 = \lambda_W^{(upp)} - \frac{\gamma}{2}\sqrt{\frac{A}{\beta}}|N_2 - N_1| \\ \frac{2}{3}\frac{\beta}{A}\frac{q_1}{\gamma^2}\left(\lambda_W^{(upp)}\right)^3 + \frac{\alpha_G - \eta}{\alpha_G}\lambda_W^{(upp)} + \frac{\gamma}{\alpha_G}\sqrt{\frac{A}{\beta}}\left(\sigma\kappa + \frac{\eta}{2}|N_2 - N_1|\right) = 0. \end{cases} \tag{49}$$

In this case, the behavior of the DW velocity close to the threshold is more complicated and requires some further details. In particular, since the breakdown conditions correspond to the positive real roots of the third-order algebraic Eqs. (48), (49), more than one value for $u_W^{(low)}$ and $u_W^{(upp)}$ could be obtained. The nature and the sign of these solutions depend on the parameters and in particular on the values of the mean curvature and of the nonlinear damping coefficient.

For instance, if there are no real positive solutions for $u_W^{(low)}$, the DW velocity lies entirely below the lower breakdown so that, according to (44), no DW motion can be observed at all.

For a double positive solution for $u_W^{(low)}$, a DW motion can only take place at the unique value of the applied current $u_W^{(low)}$ with velocity $\lambda_W^{(low)}$. Finally, if two positive roots for $u_W^{(low)}$ ($u_{W_1}^{(low)} < u_{W_2}^{(low)}$) are found, then the DW motion occurs in a range of applied currents whose lower extremum is $u_{th}^* = \max\left\{u_{th}, u_{W_1}^{(low)}\right\}$. For what concerns the upper extremum u_W^* of this interval, if at least one positive root of (49) is found, being $u_{W_1}^{(upp)}$ the smallest one, then $u_W^* = \min\left\{u_{W_2}^{(low)}, u_{W_1}^{(upp)}\right\}$, otherwise $u_W^* = u_{W_2}^{(low)}$. The DW dynamics arising in this latter case is illustrated in Fig. 4 for suitable choices of the parameters. In particular, by fixing $q_1 = 0.1$, we represent the situation $u \in \left[u_{th}, u_{W_1}^{(upp)}\right]$ for flat (□) and cylindrical (◁) DWs, whereas the one with $u \in \left[u_{W_1}^{(low)}, u_{W_1}^{(upp)}\right]$ is depicted for cylindrical (△) and spherical (○) DWs. Fig. 4 also shows the case $u \in \left[u_{W_1}^{(low)}, u_{W_2}^{(low)}\right]$ for two spherical DWs having the same curvature but different nonlinear damping coefficient $q_1 = 0.75$ (⊕) and $q_1 = 1.5$ (⊖).

In passing we note that when $u_{th}^* = u_{th}$ the threshold value only depends on k, otherwise it is also affected by q_1 (as shown in the inset of Fig. 4.

Summarizing, the overall comparison among Figs. 1 and 2 and 3, 4 allows us to conclude that the DW dynamics can be characterized by significantly different features depending on the nature of the driving sources.

We also remark that the main effect of a curved DW is the introduction of a propagation threshold which has been observed for both damping models herein considered. Such a behaviour is qualitatively similar to the one investigated in [3] for

a flat DW which propagates along a ferromagnetic nanostrip whose relaxation phenomena are described through a combined viscous-dry friction mechanism. As in [3], the Walker breakdown velocity is field-independent but current-dependent.

Finally, it is interesting to notice that the existence of velocity jumps, as well as the nonlinear dependence of the DW velocity as a function of the source terms, is consistent with some previous experimental and numerical investigations [36–38].

Acknowledgments

The paper was partially supported by MIUR-PRIN 2010-11 under Project 2010ECA8P3 "DyNanoMag".

References

[1] D. Allwood, G. Xiong, M.D. Cooke, C.C. Faulkner, D. Atkinson, N. Vernier, R.P. Cowburn, Submicrometer ferromagnetic not gate and shift register, Science 296 (2002) 2003–2006.
[2] S.S.P. Parkin, M. Hayashi, L. Thomas, Magnetic domain-wall racetrack memory, Science 320 (2008) 190–194.
[3] G. Consolo, C. Curro', E. Martinez, G. Valenti, Mathematical modeling and numerical simulation of domain wall motion in magnetic nanostrips with crystallographic defects, Appl. Math. Modell. 36 (2012) 4876–4886.
[4] G. Consolo, G. Valenti, Traveling wave solutions of the one-dimensional extended Landau–Lifshitz–Gilbert equation with nonlinear dry and viscous dissipations, Acta Appl. Math. 122 (2012) 141–152.
[5] G. Consolo, E. Martinez, The effect of dry friction on domain wall dynamics:a micromagnetic study, J. Appl. Phys. 111 (2012) (07D312).
[6] S. Zhang, Z. Li, Roles of nonequilibrium conduction electrons on the magnetization dynamics of ferromagnets, Phys. Rev. Lett. 93 (2004) 127204(1)–127204(4).
[7] A. Thiaville, Y. Nakatani, J. Miltat, Y. Suzuki, Micromagnetic understanding of current-driven domain wall motion in patterned nanowires, Europhys. Lett. 69 (2005) 990–996.
[8] W. Baltensperger, J.S. Helman, Dry friction in micromagnetics, IEEE Trans. Magn. 27 (1991) 4772–4774.
[9] P. Podio-Guidugli, G. Tomassetti, On the steady motions of a flat domain wall in a ferromagnet, Eur. Phys. J. B. 26 (2002) 191–198.
[10] R. Skomski, Domain-wall curvature and coercivity in pinning type Sm–Co magnets, J. Appl. Phys. 81 (1997) 5627–5629.
[11] S. Zapperi, P. Cizeau, G. Durin, H.E. Stanley, Dynamics of a ferromagnetic domain wall: avalenches, depinning transition, and the Barkhausen effect, Phys. Rev. B 58 (1998) 6353–6366.
[12] L. Thevenard et al, Domain wall propagation in ferromagnetic semiconductors:beyond the one-dimensional model, Phys. Rev. B 83 (2011) 245211(1)–245211(9).
[13] F.B. Hagedorn, Dynamic conversion during magnetic bubble domain wall motion, J. Appl. Phys. 45 (1974) 3129–3140.
[14] A.P. Malozemoff, J.C. Slonczewski, Magnetic Domain Walls in Bubble Materials, Academic Press, 1979.
[15] J. Zhai, Theoretical velocity of domain wall motion in ferromagnets, Phys. Lett. A 242 (1998) 266–270.
[16] P. Podio-Guidugli, G. Tomassetti, On the evolution of domain walls in hard ferromagnets, SIAM J. Appl. Math. 64 (2004) 1887–1906.
[17] B.N. Filippov, F.A. Kassan-Ogly, Nonlinear dynamic structure rearrangement of vortexlike domain walls in magnetic films with in-plane anisotropy, Physica D 237 (2008) 1151–1156.
[18] T. Tainuti, C.C. Wei, Reductive perturbation method in nonlinear wave propagation, J. Phys. Soc. Jpn. 24 (1968) 941–946.
[19] P. Germain, Progressive Waves, Jber. DGLR (1971), Koln (1972), pp. 11–39.
[20] G.B. Witham, Linear and Nonlinear Waves, Jon Wiley and Sons, New York, 1974.
[21] J.K. Hunter, J.B. Keller, Weakly nonlinear high frequency waves, Commun. Pure Appl. Math. 36 (1983) 547–569.
[22] T.L. Gilbert, A Lagrangian formulation of gyromagnetic equation of the magnetization field, Phys. Rev. 100 (1955) 1243–1255.
[23] T.L. Gilbert, A phenomenological theory of damping in ferromagnetic materials, IEEE Trans. Magn. 40 (2004) 3443–3449.
[24] V. Tiberkevich, A. Slavin, Nonlinear phenomenological model of magnetic dissipation for large precession angles: Generalization of the Gilbert model, Phys. Rev. B 75 (2007) 014440(1)–014440(6).
[25] L. Berger, Exchange interaction between ferromagnetic domain wall and electric current in very thin metallic films, J. Appl. Phys. 55 (1984) 1954–1956.
[26] L. Berger, Motion of a magnetic domain wall traversed by fast -rising current pulses, J. Appl. Phys. 71 (2002) 2721–2726.
[27] G. Tatara, H. Kohno, J. Shibata, Y. Lemaho, K.J. Lee, Spin torque and force due to current for general spin textures, J. Phys. Soc. Jpn. 76 (2007) 054707(1)–054707(13).
[28] G. Tatara, H. Kohno, Theory of current-driven domain wall motion: spin transfer versus momentum transfer, Phys. Rev. Lett. 92 (2004) 086601(1)–086601(4).
[29] Y. Tserkovnyaka, A. Brataasb, G.E.W. Bauerc, Theory of current-driven magnetization dynamics in inhomogeneous ferromagnets, J. Magn. Magn. Mater. 320 (2008) 1282–1292.
[30] G. Bertotti, Hysteresis in Magnetism, Academic Press, London, 1998.
[31] D.X. Chen, E. Pardo, A. Sanchez, Demagnetizing factors of rectangular prisms and ellipsoids, IEEE Trans. Magn. 38 (2002) 1742–1752.
[32] J.A Osborn, Demagnetizing factors of the general ellipsoid, Phys. Rev. 67 (1945) 351–357.
[33] G. Consolo, G. Gubbiotti, L. Giovannini, R. Zivieri, Lagrangian formulation of the linear autonomous magnetization dynamics in spin-torque auto-oscillators, Appl. Math. Comput. 217 (2011) 8204–8215.
[34] N.L. Schryer, I.R. Walker, The motion of 180° domain walls in uniform dc magnetic fields, J. Appl. Phys. 45 (1974) 5406–5421.
[35] C. Melcher, Domain wall motion in ferromagnetic layers, Physica D 192 (2004) 249–264.
[36] E. Martinez, L. Lopez-Diaz, L. Torres, C. Tristan, Thermal effects in domain wall motions: micromagnetic simulations and analytical model, Phys. Rev. B 75 (2007) 174409(1)–174409(11).
[37] G. Tatara, H. Kohno, J. Shibata, Microscopic approach to current-driven domain wall dynamics, Phys. Rep. 468 (2008) 213–301.
[38] S. Fukami, T. Suzuki, Y. Nakatani, N. Ishiwata, M. Yamanouchi, S. Ikeda, N. Kasai, H. Ohno, Current-induced domain wall motion in perpendicularly magnetized CoFeB nanowire, Appl. Phys. Lett. 98 (2011) 082504(1)–082504(3).